Supporting Information

Crystal Structure of the Phosphotransferase Domain of the Bifunctional Aminoglycoside Resistance Enzyme AAC(6')-Ie-APH(2")-Ia

Clyde A. Smith,[a*] Marta Toth,[b] Monolekha Bhattacharya,[b] Hilary Frase,[b] and Sergei B. Vakulenko[b*]

[a] Stanford Synchrotron Radiation Lightsource, Stanford University, Menlo Park, CA 94025

[b] Department of Chemistry and Biochemistry, University of Notre Dame, Notre Dame, IN 46556

[*] To whom correspondence should be addressed:

Dr Clyde Smith, Ph: 650-926-8544, Fax: 650-926-3292, E-mail: csmith@slac.stanford.edu

Dr Sergei B. Vakulenko, Ph: 574-631-2935, Fax: 574-631-6652, E-mail: svakulen@nd.edu

Supporting Information contents:

Supplementary Results

Space group determination and oligomerization of APH(2")-Ia

Initial indications from the native APH(2")-Ia diffraction images suggested that space group was either C222 or $C222_1$ with cell dimensions a = 110.02 Å, b = 144.21 Å and c = 95.70 Å. However, during data processing with *XDS* (Kabsch, 2010), analysis of the symmetry-related intensities gave redundancy-independent R-factors (R_{meas}) (Diederichs & Karplus, 1997) of 48.3% for this C-centered orthorhombic cell, and a significantly lower value (4.9%) for a primitive monoclinic cell with unit cell dimensions a = 90.68 Å, b = 95.70 Å, c = 91.15 Å, β = 104.9°. Systematic absences showed the presence of a two-fold screw axis, indicating that the crystal belonged to space group $P2_1$, and a Mathews coefficient (Matthews, 1968) of 2.53 $Å^3$/Da (51.5% solvent) indicated that there were four molecules in the asymmetric unit. Calculation of a self-rotation function using *POLARRFN* from the CCP4 suite (Winn *et al.*, 2011) also reveals the presence of this orthorhombic pseudosymmetry.

The four molecules in the asymmetric unit are related by two orthogonal two-fold axes, each lying roughly parallel to the diagonals of the *ab*-plane. One of the non-crystallographic two-fold axes relates two pairs of monomers, monomer A with monomer D, and monomer B with monomer C (Figure S2), with approximately 900 $Å^2$ of surface area per monomer buried upon formation. The second two-fold axis then maps the AD dimer onto the BC dimer to generate a dimer of dimers, burying approximately 2400 $Å^2$ of surface area per dimer. The two dimers are offset from one another by about 22 Å along a vector almost parallel with the *c** axis.

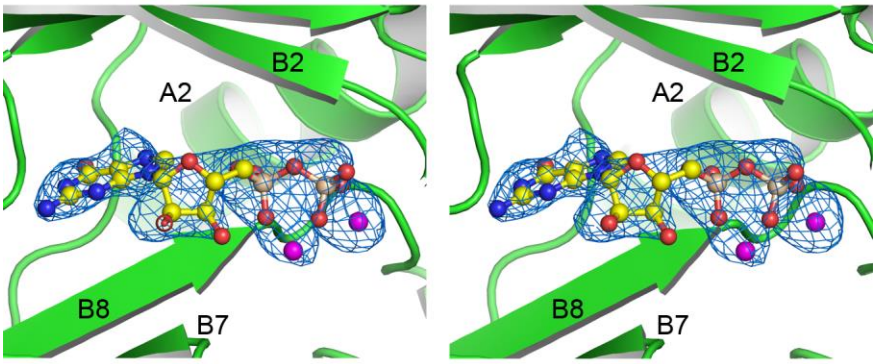

Figure S1: Stereoview of the experimental $2F_o$-F_c electron density (contoured at 2.8 σ) in the nucleotide binding site prior to structure refinement. The final model for the enzyme is shown in cartoon representation (green), and the GDP from the final refinement model is shown as yellow ball-and-stick. The two lobes of density adjacent to the diphosphate moiety represents the two magnesium ions which are also shown from the final model.

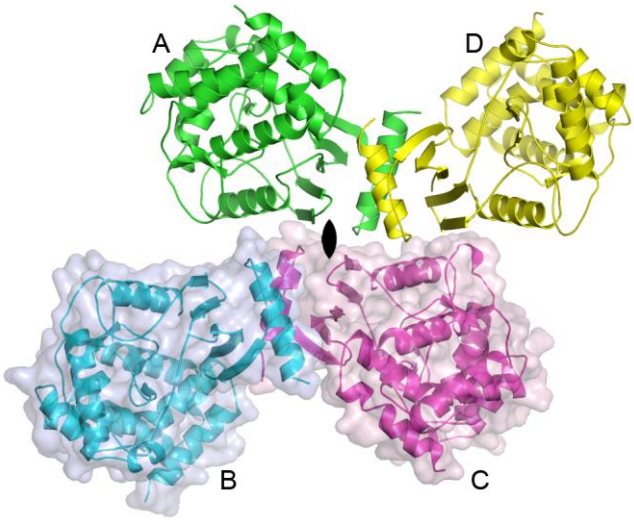

Figure S2: Oligomeric structure of APH(2")-Ia. The four independent molecules in the $P2_1$ asymmetric unit, shown as a dimer of dimers. The upper dimer (A, green and D, yellow) is related to the lower dimer (B, blue and C, red, shown in a transparent molecule surface) by a non-crystallographic dyad.

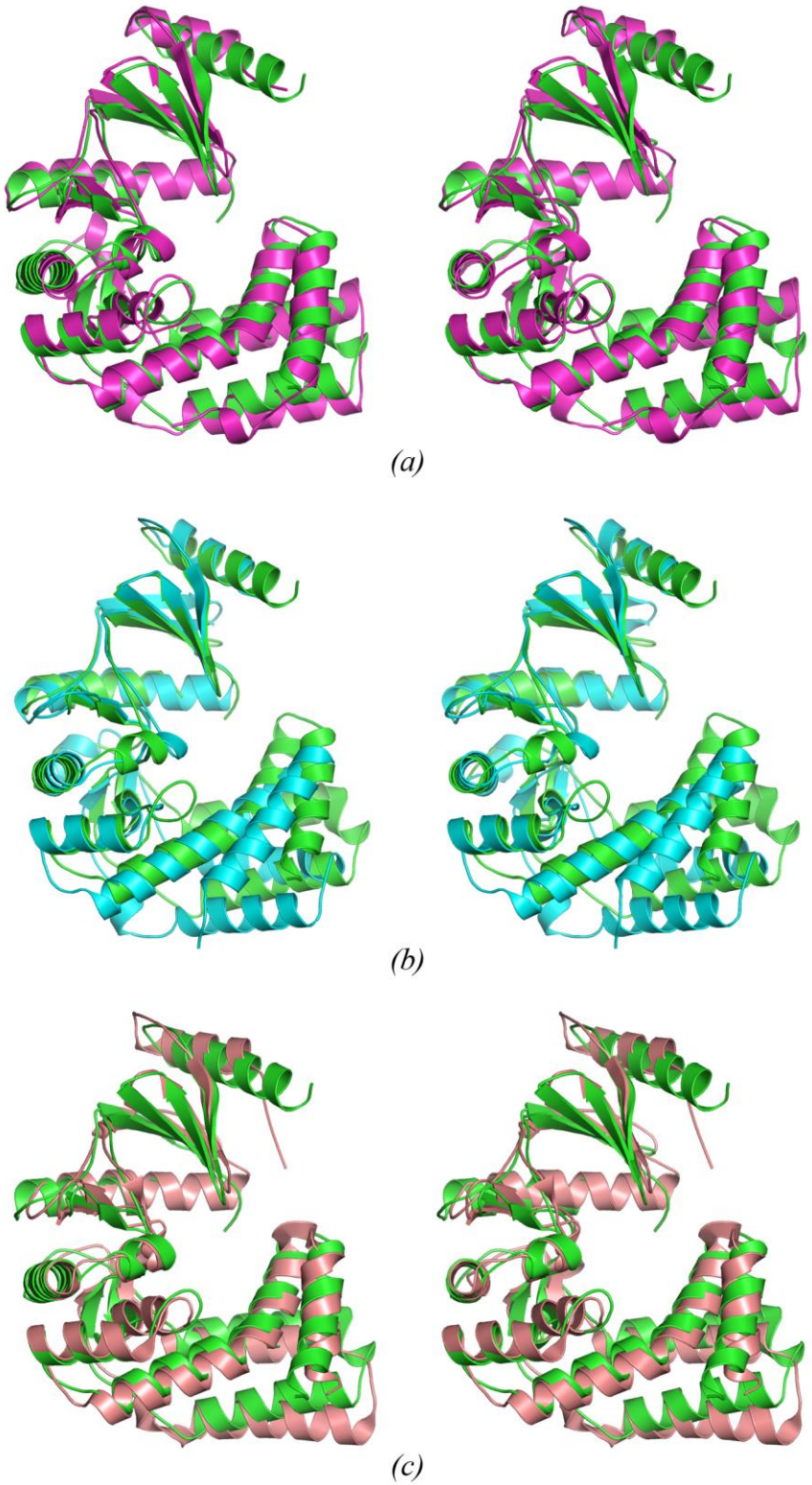

Figure S3: Comparison of APH(2”)-Ia with other APH(2”) enzymes. Stereoviews of the superpositions of *(a)* APH(2”)-Ia (green) and APH(2”)-IIa (magenta). *(b)* APH(2”)-Ia (green)

and APH(2”)-IIIa (cyan). *(c)* APH(2”)-Ia (green) and APH(2”)-IVa (salmon). The same color scheme for the APH(2”) enzymes will be used throughout.

Table S1

The *rms* differences between APH(2”)-Ia and the other three APH(2”) enzymes

Numbers in parentheses indicate the number of matching Cα atoms. The *rmsd*s are given in Å.

	APH(2”)-IIa	APH(2”)-IIIa	APH(2”)-IVa
Sequence identity (%)	30.1	23.9	29.3
All[†]	2.1 (268)	3.0 (270)	1.9 (273)
N-domain	1.2 (67)	0.8 (63)	1.0 (62)
Core sub-domain	1.0 (88)	1.0 (72)	1.0 (98)
Helical sub-domain[‡]	2.1 (77)	2.0 (64)	1.6 (74)
A6/A7	1.9 (35)	1.2 (27)	1.5 (33)
A10/A11	1.1 (42)	1.7 (37)	0.9 (41)
N+core+helical[§]	1.9 (232)	2.8 (199)	1.7 (234)

[†] Calculated using the SSM algorithm (Krissinel & Henrick, 2004) implemented in *COOT* (Emsley & Cowtan, 2004).

[‡] The first number refers to all four helices superimposed as a rigid body.

[§] Calculated with *LSQKAB* from the CCP4 suite (Winn *et al.*, 2011) with the same residue matches used for the individual N-domain, core and helical sub-domain superpositions.

References

Diederichs, K. & Karplus, P. A. (1997). *Nature Struct. Biol.* **4**.

Emsley, P. & Cowtan, K. (2004). *Acta Crystallogr.* **D60**, 2126-2132.

Kabsch, W. (2010). *Acta Crystallogr.* **D66**, 133-144.

Krissinel, E. & Henrick, K. (2004). *Acta Crystallogr.* **D60**, 2256–2268.

Matthews, B. W. (1968). *Journal of Molecular Biology* **33**, 491-497.

Winn, M. D., Ballard, C. C., Cowtan, K. D., Dodson, E. J., Emsley, P., Evans, P. R., Keegan, R. M., Krissinel, E. B., Leslie, A. G. W., McCoy, A., McNicholas, S. J., Murshudov, G. N., Pannu, N. S., Potterton, E. A., Powell, H. R., Read, R. J., Alexei Vagin, A. & Wilson, K. S. (2011). *Acta Cryst.* **D67**, 235-242.